NJC

PAPER

View Article Online
View Journal | View Issue

Cite this: *New J. Chem.*, 2014, **38**, 6198

A highly selective turn-on fluorescent sensor for fluoride and its application in imaging of living cells†

Jiun-Ting Yeh, Parthiban Venkatesan and Shu-Pao Wu*

Received (in Montpellier, France) 3rd September 2014,
Accepted 26th September 2014

DOI: 10.1039/c4nj01486c

www.rsc.org/njc

A fluorescent probe (**FS**) based on a fluoride-specific desilylation reaction has been developed for a highly selective and sensitive detection of F^-. In the presence of F^-, the probe **FS** provided significant green fluorescence enhancement, while other anions produced only minor changes in fluorescence intensity. The probe **FS** has a limit of detection of 1.45 μM, which is reasonable for the detection of micromolar concentrations of F^- ions. The maximum fluorescence enhancement induced by F^- in the probe was observed over the pH range 7–10. Moreover, fluorescence microscopy imaging using mouse leukaemic monocyte macrophage showed that the probe **FS** could be an efficient fluorescent probe for F^- ions in living cells.

1. Introduction

The development of sensors for biologically important anions is currently an important research focus because of their important roles in various biological processes.[1–5] Fluoride is a useful additive in toothpaste and in drinking water for the prevention of dental caries. However, excess of fluoride can result in fluorosis, urolithiasis, and cancer.[6–11] Therefore, precise determination of fluoride in samples is necessary. Up to now, several methods such as ion chromatography,[12,13] ion-selective electrode,[14] and the Willard and Winter methods[15] have been used for quantitative fluoride detection. On the other hand, these methods have some disadvantages such as high costs and complicated procedures. Now, more attention has focused on the development of highly selective and convenient methods for fluoride detection.

A large number of fluorescent probes have been developed for fluoride detection based on three molecular interactions: hydrogen bonding between fluoride and NH hydrogen (amide, indole, pyrrole, thiourea, and urea),[16–26] boron–fluoride complexation,[27–30] and fluoride-mediated desilylation.[31–35] Because fluoride ions have strong tendency for hydration, the approach using hydrogen bonding is not applicable in aqueous media. The fluoride-mediated desilylation strategy does not have such limitations and can provide the best way for detecting fluoride in aqueous solution. In this study, a coumarin derivative with the Si–O functionality was used for the detection of fluoride anions in living cells.

In this study, we designed a fluorescent chemosensor **FS** for fluoride detection. The chemosensor comprises two parts: a Si–O functionality and a coumarin derivative. F^- triggers cleavage of the Si–O bond, leading to the strong green emission of the coumarin derivative. We have performed a competitive analysis for F^- ions with other anions such as Br^-, CN^-, Cl^-, $H_2PO_4^-$, I^-, NO_2^-, NO_3^-, N_3^-, OAc^-, and $P_2O_7^{4-}$ with **FS**. The result shows that F^- is the only anion that triggers the cleavage of the Si–O bond in **FS** and that it causes the formation of a strongly fluorescent green derivative while other anions do not. This new probe exhibits high selectivity and sensitivity toward F^- over other anions in aqueous solutions. Most importantly, **FS** shows good permeability for cell membranes and is applicable to F^- imaging of living cells.

2. Experimental section

2.1 Materials and instrumentation

All solvents and reagents were obtained from commercial sources and used as received without further purification. UV/Vis spectra were recorded on an Agilent 8453 UV/Vis spectrometer. NMR spectra were obtained on a Bruker DRX-300 and Agilent Unity INOVA-500 NMR spectrometer. IR data were obtained on a Bomem DA8.3 Fourier-Transform Infrared Spectrometer. Fluorescence spectra measurements were performed on a Hitachi F-7000 fluorescence spectrophotometer. Fluorescent images were taken on a Leica TCS SP5 X AOBS confocal fluorescence microscope.

2.2 Synthesis of 2-((*tert*-butyldiphenylsilyl)oxy)-4-(diethylamino)-benzaldehyde (1)

4-Diethylaminosalicyl aldehyde (193 mg, 1.00 mmol), imidazole (100 mg, 1.47 mmol) and *tert*-butyldiphenylchlorosilane

Department of Applied Chemistry, National Chiao Tung University, Hsinchu, Taiwan 300, Republic of China. E-mail: spwu@mail.nctu.edu.tw; Fax: +886-3-5723764; Tel: +886-3-5712121 ext 56506

† Electronic supplementary information (ESI) available: ^1H and ^{13}C NMR spectra of **FS**, calibration curve of **FS** with F^-. See DOI: 10.1039/c4nj01486c

(275 μL, 1.0 mmol) were dissolved in DMF (1 mL). The mixture was stirred at 50 °C for 12 h. The solvent was removed under reduced pressure, and the crude product was purified using column chromatography (hexane : ethyl acetate = 4 : 1) to give the compound as a white solid. Yield: 384 mg (89.2%). Melting point: 108–109 °C. ^{1}H-NMR (300 MHz, $CDCl_3$): δ 10.49 (s, 1H), 7.77–7.78 (m, 5H), 7.37–7.44 (m, 6H), 6.22 (d, J = 9.0 Hz, 1H), 5.59 (s, 1H), 2.93 (q, J = 6.6 Hz, 4H), 1.13 (s, 9H), 0.76 (t, J = 6.9 Hz, 6H); ^{13}C-NMR (125 MHz, $CDCl_3$): δ 187.2, 160.8, 153.1, 135.3, 132.3, 130.0, 129.8, 127.9, 115.6, 105.2, 100.9, 44.4, 26.5, 19.6, 12.1. MS (EI): m/z (%) = 431 (6.4), 374 (100), 354 (1.7), 330 (12.9), 224 (2.1); HRMS (EI): calcd for $C_{36}H_{37}N_3OSSi$ (M^+) 431.2281; found, 431.2277.

2.3 Synthesis of (*E*)-2-(benzo[*d*]thiazol-2-yl)-3-(2-((*tert*-butyldiphenylsilyl)oxy)-4-(diethylamino)phenyl)acrylonitrile (FS)

To the solution of 1,3-benzothiazol-2-ylacetonitrile (87 mg, 0.5 mmol) dissolved in 10 mL methanol, piperidine (150 μL) was added and stirred for 5 min. 2-((*tert*-Butyldiphenylsilyl)oxy)-4-(diethylamino)benzaldehyde was added to the mixture, and stirred at room temperature overnight. An orange precipitate was formed, and the crude product was filtered, and thoroughly washed with methanol to give the compound **FS**. Yield, 41 mg (14.0%). Melting point: 197–198 °C. ^{1}H-NMR (300 MHz, $CDCl_3$): δ 8.88 (s, 1H), 8.49 (d, J = 9.3 Hz, 1H), 8.03 (d, J = 8.1 Hz, 1H), 7.87 (d, J = 7.8 Hz, 1H), 7.78–7.80 (m, 4H), 7.34–7.51 (m, 8H), 6.33 (dd, J = 9.3 Hz, J = 1.8 Hz, 1H), 5.70 (d, J = 1.8 Hz, 1H), 2.98 (q, J = 6.9 Hz, 4H), 1.25 (s, 9H) 0.80 (t, J = 7.2 Hz, 6H); ^{13}C-NMR (125 MHz, $CDCl_3$): δ 165.9, 158.0, 154.0, 151.9, 141.5, 135.4, 134.3, 132.1, 130.2, 128.0, 126.3, 124.8, 122.9, 121.2, 118.5, 111.3, 105.9, 101.4, 96.1, 44.6, 26.7, 19.7, 12.3. IR (KBr): 2969, 2927, 2854, 2212, 1609, 1591, 1559 cm^{-1}. MS (EI): m/z (%) = 587(97.3), 530(100); HRMS (EI): calcd for $C_{36}H_{37}N_3OSSi$ (M^+) 587.2427; found, 587.2420.

2.4 Anion selection study using fluorescence spectroscopy

The chemosensor **FS** (10 μM) was added with different anions (1 mM). All spectra were measured in 1.0 mL acetonitrile–water solution (v/v = 1 : 1, 10 mM HEPES, pH 7.0). The light path length of the cuvette was 1.0 cm.

2.5 The pH dependence on the reaction of the fluoride with the chemosensor FS using fluorescence spectroscopy

Chemosensor **FS** (10 μM) was added with F^- (20 μM) in 1.0 mL acetonitrile–water solution (v/v = 1 : 1, 10 mM buffer). The buffers were: pH 3–4, KH_2PO_4–HCl; pH 4.5–6, KH_2PO_4–NaOH; pH 6.5–8.5, HEPES; pH 9–10, Tris-HCl.

2.6 Cell culture

RAW 264.7 cells were cultured in Dulbecco's modified Eagle's medium (DMEM) supplemented with 10% fetal bovine serum (FBS) at 37 °C under an atmosphere of 5% CO_2. Cells were plated on 18 mm glass coverslips and allowed to adhere for 24 h.

2.7 Cytotoxicity assay

The methyl thiazolyl tetrazolium (MTT) assay was used to measure the cytotoxicity of **FS** in RAW264.7 cells. RAW264.7 cells were seeded into a 96-well cell-culture plate. Various concentrations

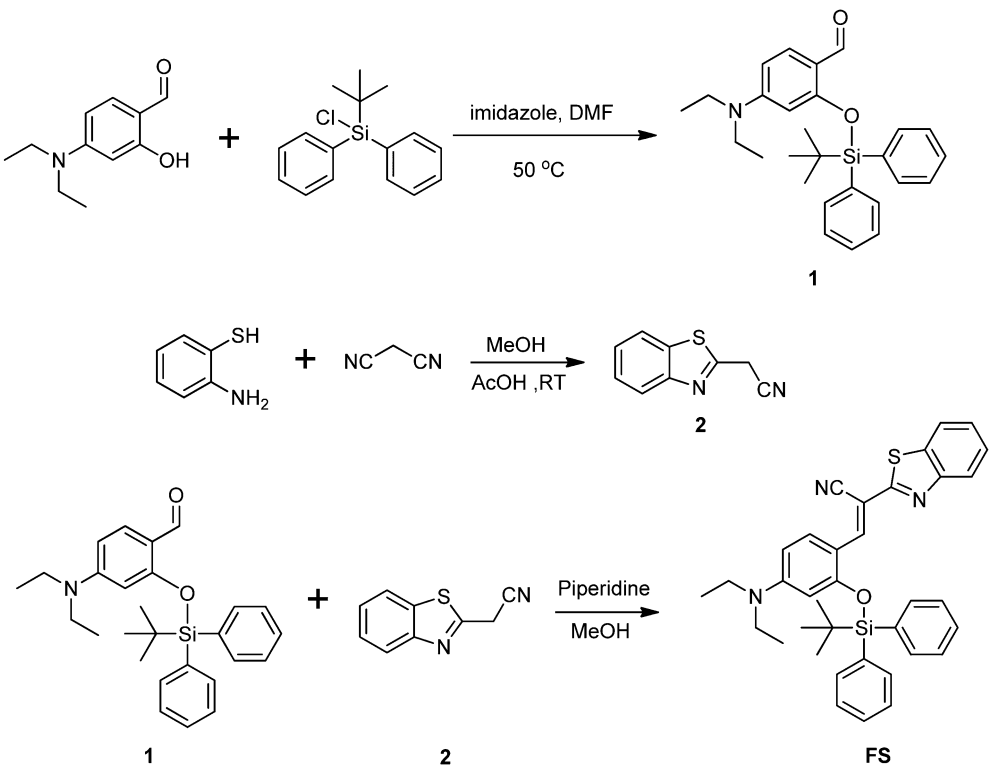

Scheme 1 Synthesis of chemosensor **FS**.

(5, 10, 15, 20, 25 μM) of **FS** were added to the wells. The cells were incubated at 37 °C under 5% CO_2 for 24 h. 10 μL MTT (5 mg mL^{-1}) was added to each well and incubated at 37 °C under 5% CO_2 for 4 h. Remove the MTT solution and yellow precipitates (formazan) observed in plates were dissolved in 200 μL DMSO and 25 μL Sorenson's glycine buffer (0.1 M glycine and 0.1 M NaCl). A Multiskan GO microplate reader was used to measure the absorbance at 570 nm for each well. The viability of cells was calculated according to the following equation:

Cell viability (%) = (mean of absorbance value of treatment group)/(mean of absorbance value of control group).

2.8 Cell imaging

Experiments to assess the F^- uptake were performed in phosphate-buffered saline (PBS) with 20 μM NaF. The cells cultured in DMEM were treated with 10 mM solutions of NaF (2 μL; final concentration: 20 μM) dissolved in sterilized PBS (pH = 7.4) and incubated at 37 °C for 30 min. The treated cells were washed with PBS (3 × 2 mL) to remove remaining metal ions. DMEM (2 mL) was added to the cell culture, which was then treated with a 10 mM solution of chemosensor **FS** (2 μL; final concentration: 20 μM) dissolved in DMSO. The samples were incubated at 37 °C for 30 min. The culture medium was removed, and the treated cells were washed with PBS (3 × 2 mL) before observation. Confocal fluorescence imaging of cells was performed with a Leica TCS SP5 X AOBS confocal fluorescence microscope (Germany), and a 63× oil-immersion objective lens was used. The cells were excited with a white light laser at 480 nm, and emission was collected at 535 ± 10 nm.

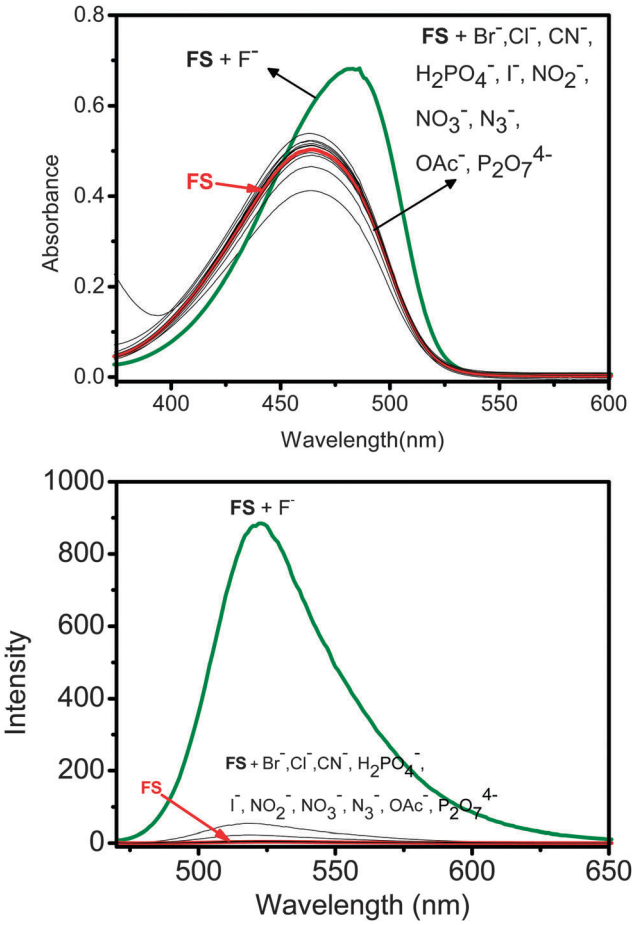

Fig. 2 UV-Vis (top) and fluorescence (bottom) spectra of **FS** (10.0 μM) in acetonitrile–water (v/v = 1 : 1, (C)10 mM HEPES, pH 7.0) solution, after the addition of various anions (1 mM). The excitation wavelength was 465 nm.

3. Results and discussion

3.1 Synthesis of the probe FS

The synthesis of the probe **FS** is outlined in Scheme 1. 4-Diethylaminosalicyl aldehyde and *tert*-butyldiphenylchlorosilane were reacted to form 2-((*tert*-butyldiphenylsilyl)oxy)-4-(diethylamino) benzaldehyde. Further reaction of 2-((*tert*-butyldiphenylsilyl)oxy)-4-(diethylamino) benzaldehyde with 1,3-benzothiazol-2-ylacetonitrile

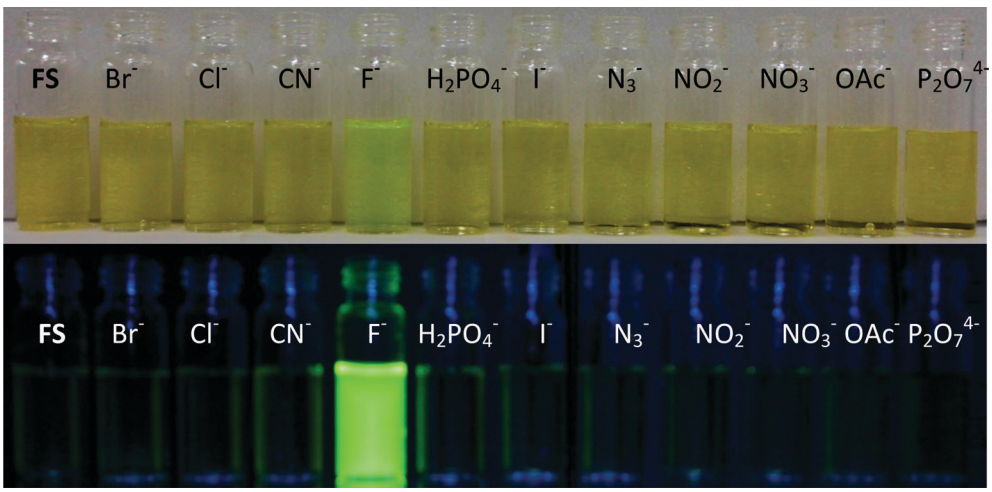

Fig. 1 Color (top) and fluorescence (bottom) changes in **FS** upon the addition of various anions in a acetonitrile–water (v/v = 1 : 1, 10 mM HEPES, pH 7.0) solution.

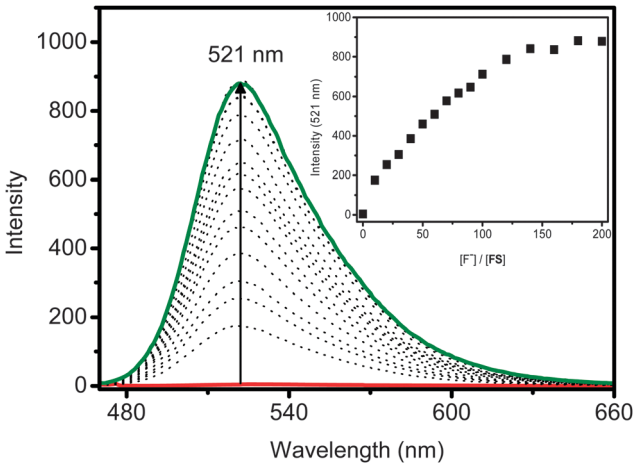

Fig. 3 Emission spectra of **FS** (10 μM) in acetonitrile–water (v/v = 1 : 1, 10 mM HEPES, pH 7.0) solution upon the addition of 0–2 mM of F^-. The excitation wavelength was 465 nm. The incubation time was 180 minutes.

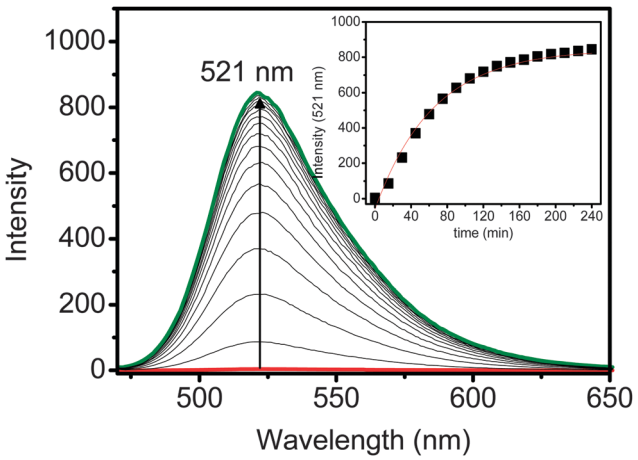

Fig. 4 Time-course measurement of the fluorescence response of **FS** (10 μM) to F^- (1 mM). The excitation wavelength was 465 nm.

in equimolar quantities yields the chemosensor **FS** (Scheme 1). **FS** is yellow and has an absorption band centered at 465 nm with a quantum yield (Φ) of 0.001.

3.2 Anion-sensing properties

To evaluate the selectivity of the chemosensor **FS** toward various anions, absorption spectra and fluorescence spectra of **FS** were measured in the presence of 12 anions: F^-, Br^-, Cl^-, CN^-, $H_2PO_4^-$, HSO_3^-, I^-, N_3^-, NO_2^-, NO_3^-, OAc^-, and $P_2O_7^{4-}$ (Fig. 1). Only F^- caused a visible color change in **FS** (yellow to green) and had a green emission (Fig. 1). Fig. 2 shows the absorption spectra and fluorescence spectra of **FS** with various anions. Addition of F^- caused the absorption band at 465 nm to shift to 483 nm and formation of a new emission band centered at 521 nm. Fig. 3 shows the titration of F^- with the chemosensor **FS**. After addition of 100 equivalents of F^-, the emission intensity reached a maximum. The quantum yield of the new emission band was 0.146, which is 146-fold that of the chemosensor **FS** at 0.001. The fluoride ion was the only anion that we tested that readily reacted with **FS** to yield a significant fluorescence enhancement, suggesting the possibility of application for the highly selective detection of F^- ions. The limit of detection for the chemosensor **FS** as a fluorescent sensor for F^- detection was determined from a plot of fluorescence intensity as a function of F^- concentration (see Fig. S7 in the ESI†). We found that the chemosensor **FS** has a limit of detection of 1.45 μM, which is reasonable for the detection of micromolar concentrations of F^- ions.

The time course for the reaction of the chemosensor **FS** with fluoride is shown in Fig. 4. The pseudo-first-order condition (10 μM **FS**, 1 mM F^-) was employed. By fitting the time course, the observed rate constant for F^- deprotection of **FS** was found to be 0.0155 min^{-1}. The mechanism of fluoride-mediated desilylation is shown in Scheme 2. F^- triggers the cleavage of the Si–O bond in **FS**, and then phenol attacks the cyano group to form a cyclic coumarin derivative with a strong green emission. To confirm the

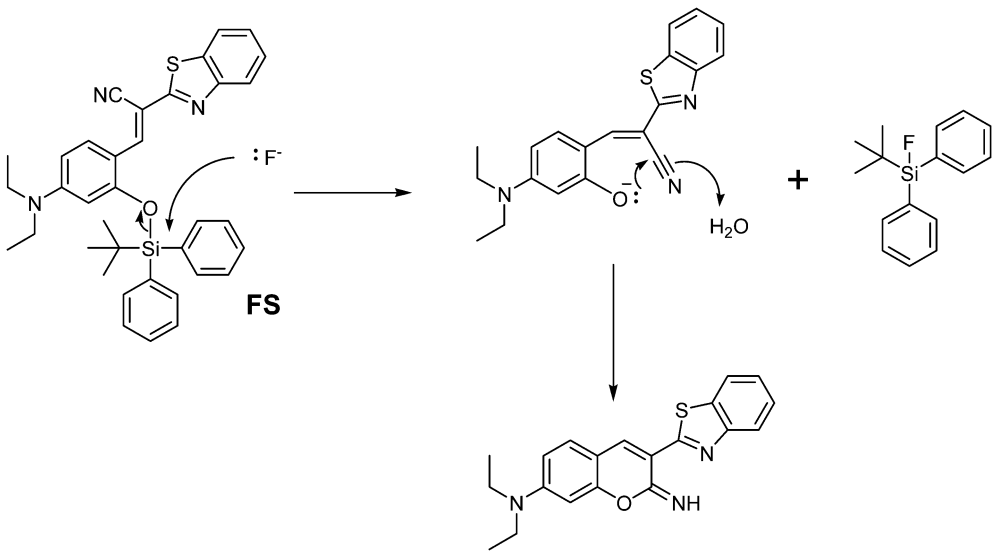

Scheme 2 The reaction mechanism of **FS** and F^-.

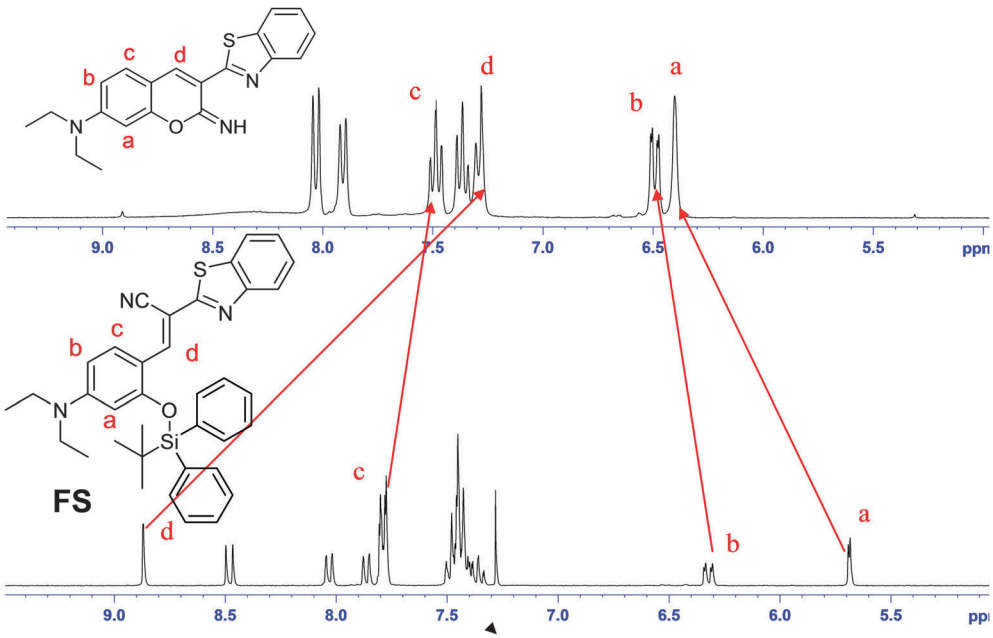

Fig. 5 ^{1}H NMR spectral change of the reaction of **FS** with NaF in $CDCl_3$.

formation of the coumarin ring through the reaction of **FS** with NaF, ^{1}H NMR spectroscopy (Fig. 5) was employed. After the reaction with F^-, the imine proton (δ 8.88 ppm, H_d) of **FS** showed upfield shifts due to the formation of a cyclic coumarin derivative. The proton signals (H_a and H_b) in the phenyl ring showed downfield shifts after the reaction. These observations support the formation of the coumarin ring.

To study the influence of other anions on the reaction of F^- with the chemosensor **FS**, we performed competitive experiments with other anions (1 mM) in the presence of F^- (1 mM) (Fig. 6). The observed fluorescence enhancement for mixtures of F^- with most anions was similar to that seen for F^- alone. We observed high fluorescence enhancement only with mixtures of F^- with CN^- or $P_2O_7^{4-}$, indicating that CN^- and $P_2O_7^{4-}$ might aid the reaction of F^- with the chemosensor **FS**. No other anions appeared to interfere with the fluorescence of the chemosensor **FS** and F^-.

We performed pH titration of the chemosensor **FS** to investigate a suitable pH range for the reaction of F^- with the chemosensor **FS**. As shown in Fig. 7, the emission intensities of the chemosensor **FS** are very low. After mixing of **FS** with F^- in the pH range 7–10, the emission intensity at 521 nm rapidly increases to a maximum. At pH $<$ 6, the enhanced emission does not occur because of protonation of F^-, preventing fluoride-mediated desilylation.

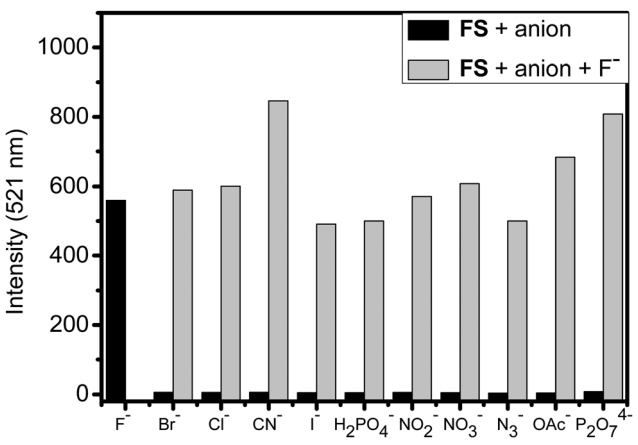

Fig. 6 Fluorescence response of chemosensor **FS** (10 μM) to F^- (1 mM) or 1 mM of other anions (the black bar portion) and to the mixture of other anions (1 mM) with 1 mM of F^- (the gray bar portion) in acetonitrile–water (v/v = 1 : 1, 10 mM HEPES, pH 7.0) solution.

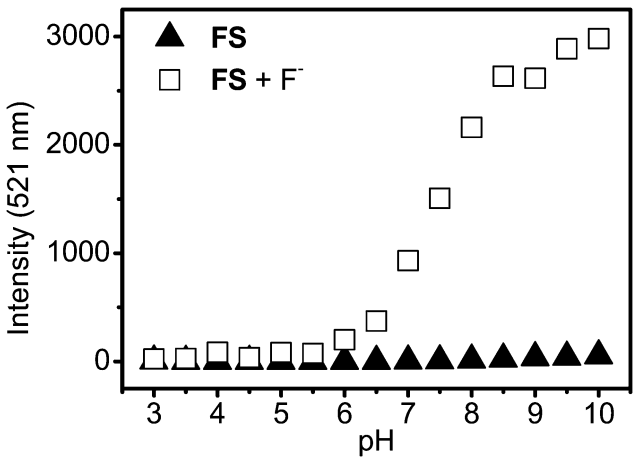

Fig. 7 Fluorescence response of free chemosensor **FS** (10 μM) (▲) and after addition of F^- (1 mM) (□) in acetonitrile–water (v/v = 1 : 1, 10 mM buffer, pH 3–4: PBS, pH 4.5–6: MES, pH 6.5–8.5: HEPES, pH 9–10: Tris-HCl) as a function of different pH values. The excitation wavelength was 465 nm.

3.3 Cell imaging

Finally, the potential of the probe **FS** for imaging F^- in living cells was investigated. First, an MTT assay with a RAW264.7 cell line was used to determine the cytotoxicity of **FS**. The cellular viability was estimated to be greater than 80% after 24 h, which indicates that **FS** (<30 mM) has low cytotoxicity (Fig. 8). Furthermore, images of the cells were obtained using a confocal fluorescence microscope. The cells were then incubated with the chemosensor **FS** (20 μM) for 30 min and then washed with PBS to remove any remaining sensor. Images of the RAW 264.7 cells were obtained by using a confocal fluorescence microscope. Fig. 9 shows images of RAW 264.7 cells with the chemosensor **FS** after treatment with F^-. An overlay of fluorescence images and bright-field images shows that the fluorescence signals are localized in the intracellular area, indicating subcellular distribution of F^- and good cell-membrane permeability of the chemosensor **FS**.

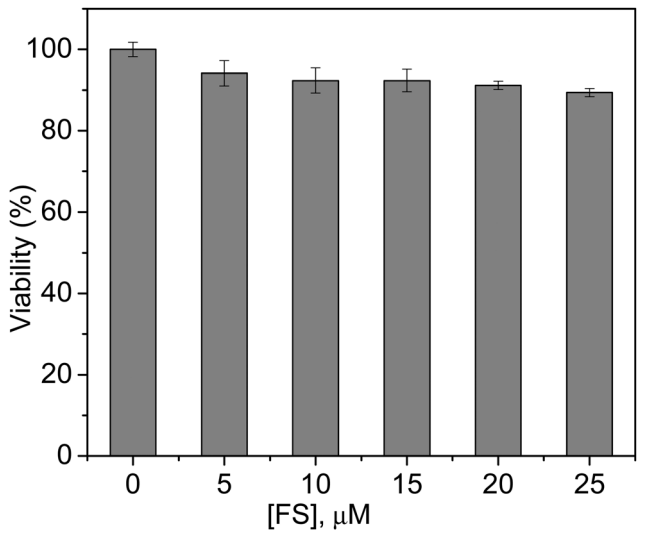

Fig. 8 Cell viability values (%) estimated by an MTT assay *versus* incubation concentrations of **FS**. RAW264.7 cells were cultured in the presence of **FS** (0–25 μM) at 37 °C for 24 h.

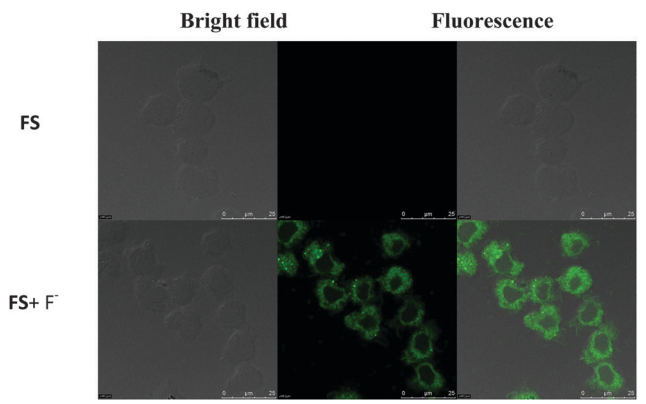

Fig. 9 Fluorescence images of macrophage (RAW 264.7) cells treated with **FS** and NaF. (left) Bright field image; (middle) fluorescence image; and (right) merged image.

4. Conclusion

In conclusion, we have reported a coumarin-based fluorescent chemosensor **FS** for F^- sensing that exhibits a turn-on response both *in vitro* and in live cells. The detection of F^- is achieved through significant fluorescence enhancement resulting from the fluoride-mediated desilylation. This probe displays high selectivity and sensitivity toward F^- over other anions in aqueous solutions. Most importantly, the chemosensor **FS** may have application in fluorescence imaging of living cells. This coumarin-based F^- chemosensor provides an effective probe for F^- sensing.

Acknowledgements

We gratefully acknowledge the financial support of Ministry of Science and Technology (Taiwan, MOST 103-2113-M-009-005).

References

1 P. A. Gale, *Chem. Soc. Rev.*, 2010, **39**, 3746–3771.
2 C. Caltagirone and P. A. Gale, *Chem. Soc. Rev.*, 2009, **38**, 520–563.
3 R. Martínez-Máñez and F. Sancenón, *Chem. Rev.*, 2003, **103**, 4419–4476.
4 M. E. Moragues, R. Martinez-Manez and F. Sancenon, *Chem. Soc. Rev.*, 2011, **40**, 2593–2643.
5 L. E. Santos-Figueroa, M. E. Moragues, E. Climent, A. Agostini, R. Martinez-Manez and F. Sancenon, *Chem. Soc. Rev.*, 2013, **42**, 3489–3613.
6 R. J. Carton, *Fluoride*, 2006, **39**, 163–172.
7 M. H. Arhima, O. P. Gulati and S. C. Sharma, *Phytother. Res.*, 2004, **18**, 244–246.
8 H. Matsui, M. Morimoto, K. Horimoto and Y. Nishimura, *Toxicol. In Vitro*, 2007, **21**, 1113–1120.
9 H. S. Horowitz, *J. Public Health Dent.*, 2003, **63**, 3–8.
10 S. Ayoob and A. K. Gupta, *Crit. Rev. Environ. Sci. Technol.*, 2006, **36**, 433–487.
11 E. Bassin, D. Wypij, R. Davis and M. Mittleman, *Cancer Causes Control*, 2006, **17**, 421–428.
12 M. A. G. T. van den Hoop, R. F. M. J. Cleven, J. J. van Staden and J. Neele, *J. Chromatogr. A*, 1996, **739**, 241–248.
13 R. I. Stefan, J. F. van Staden and H. Y. Aboul-Enein, *Pharm. Acta Helv.*, 1999, **73**, 307–310.
14 R. DeMarco, G. Clarke and B. Pejcic, *Electroanalysis*, 2007, **19**, 1987–2001.
15 W. D. Armstrong, *J. Am. Chem. Soc.*, 1933, **55**, 1741–1742.
16 Y. Qu, J. Hua and H. Tian, *Org. Lett.*, 2010, **12**, 3320–3323.
17 M. Vázquez, L. Fabbrizzi, A. Taglietti, R. M. Pedrido, A. M. González-Noya and M. R. Bermejo, *Angew. Chem., Int. Ed.*, 2004, **43**, 1962–1965.
18 K. J. Chang, D. Moon, M. S. Lah and K. S. Jeong, *Angew. Chem., Int. Ed.*, 2005, **44**, 7926–7929.
19 M. Boiocchi, L. Del Boca, D. E. Gómez, L. Fabbrizzi, M. Licchelli and E. Monzani, *J. Am. Chem. Soc.*, 2004, **126**, 16507–16514.
20 A. S. F. Farinha, M. R. C. Fernandes and A. C. Tomé, *Sens. Actuators, B*, 2014, **200**, 332–338.

21 B. Deka and R. J. Sarma, *Sens. Actuators, B*, 2014, **197**, 321–325.
22 U. N. Yadav, P. Pant, D. Sharma, S. K. Sahoo and G. S. Shankarling, *Sens. Actuators, B*, 2014, **197**, 73–80.
23 V. Luxami, A. S. Gupta and K. Paul, *New J. Chem.*, 2014, **38**, 2841–2846.
24 R. Liu, Y. Gao, Q. Zhang, X. Yang, X. Lu, Z. Ke, W. Zhou and J. Qu, *New J. Chem.*, 2014, **38**, 2941–2945.
25 X. Yong, M. Su, W. Wan, W. You, X. Lu, J. Qu and R. Liu, *New J. Chem.*, 2013, **37**, 1591–1594.
26 Madhuprasad, N. Swathi, J. R. Manjunatha, U. K. Das, A. N. Shetty and D. R. Trivedi, *New J. Chem.*, 2014, **38**, 1484–1492.
27 Z. Q. Liu, M. Shi, F. Y. Li, Q. Fang, Z. H. Chen and T. Yi, *Org. Lett.*, 2005, **7**, 5481–5484.
28 C. W. Chiu and F. P. Gabbaï, *J. Am. Chem. Soc.*, 2006, **128**, 14248–14249.
29 X. Y. Liu, D. R. Bai and S. Wang, *Angew. Chem., Int. Ed.*, 2006, **45**, 5475–5478.
30 X. Liu, M. Mao, M. Ren, Y. Tong and Q. Song, *Sens. Actuators, B*, 2014, **200**, 317–324.
31 R. Hu, J. Feng, D. Hu, S. Wang, S. Li, Y. Li and G. Yang, *Angew. Chem., Int. Ed.*, 2010, **49**, 4915–4918.
32 J. F. Zhang, C. S. Lim, S. Bhuniya, B. R. Cho and J. S. Kim, *Org. Lett.*, 2011, **13**, 1190–1193.
33 P. Sokkalingam and C. H. Lee, *J. Org. Chem.*, 2011, **76**, 3820–3828.
34 B. Zhu, F. Yuan, R. Li, Y. Li, Q. Wei, Z. Ma, B. Du and X. Zhang, *Chem. Commun.*, 2011, **47**, 7098–7100.
35 X. Cheng, H. Jia, J. Feng, J. Qin and Z. Li, *Sens. Actuators, B*, 2014, **199**, 54–61.

